

The Zintl Phases $\text{Sr}_{2.2}\text{Mg}_{11.8}\text{Ge}_7$ and $\text{Sr}_5\text{Mg}_{19}\text{Ge}_{12}$

SHARON J. STEINWAND, WEIR-MIRN HURNG, AND JOHN D. CORBETT

Department of Chemistry and Ames Laboratory–DOE,
Iowa State University, Ames, Iowa 50011 USA*

Received February 12, 1991; in revised form April 18, 1991

Synthetic investigations of the $\text{Sr}_x\text{Mg}_{2-x}\text{Ge}$ section have been carried out in sealed Ta containers. These reveal, in addition to the known Mg_2Ge , MgSrGe , and Sr_2Ge , two new phases with the nominal compositions $\text{Sr}_{2.2}\text{Mg}_{11.8}\text{Ge}_7$ and $\text{Sr}_5\text{Mg}_{19}\text{Ge}_{12}$. The first is a line compound that is isostructural with $\text{Zr}_2\text{Fe}_{12}\text{P}_7$ ($P6$, $Z = 1$, $a = 11.064$ (1) Å, $c = 4.356$ (1) Å; $R, R_w(F) = 2.7, 4.2\%$) and has the refined composition $\text{Sr}_{2.17(2)}\text{Mg}_{11.83(2)}\text{Ge}_7$. About 6% strontium substitutes in the larger, five-coordinate magnesium site. The other phase is isostructural with $\text{Ho}_5\text{Ni}_{19}\text{P}_{12}$ or the very similar $\text{Sc}_5\text{Co}_{19}\text{P}_{12}$ according to Guinier powder diffraction and is nonstoichiometric, viz., $\text{Sr}_{5+y}\text{Mg}_{19-y}\text{Ge}_{12}$ with an approximate range of $-0.7 \leq y \leq 2.7$. Both structures feature tricapped trigonal prismatic units of metal about isolated germanium atoms, these prisms being condensed by sharing some prismatic edges and faces. The new compounds are the first valence (Zintl) examples of structures previously known only for metallic transition-metal phosphides and arsenides. © 1991 Academic Press, Inc.

Introduction

A closely related series of A_2X compounds exists in which A is a group II metal Mg, Ca, Sr, or Ba and X comes from the silicon family, Si, Ge, or Sn especially. Magnesium examples of the entire series, lead included, have the cubic antiferroite structure and are some of the earliest examples of Zintl phases (1, 2) with isolated X atoms. The heavier (alkaline-earth) metals Ca–Ba all form analogous valence compounds with each member of the silicon family but in the inverse PbCl_2 (or, more distantly, Co_2Si) structure

in which nine-coordinate metalloids within tricapped trigonal prisms are condensed so as to share end faces and two-thirds of the side edges (3). Simple mixed metal examples $AA'X$ are similar, MgCaX (4), MgSrX , and CaBaX being known in this structure for the entire series of X . The group II metal (= chloride) positions are nonequivalent in this structure, and the larger metals in $AA'X$ are generally positioned in the shared side edges of the trigonal prisms while the smaller atoms are members of only one prism but in turn cap two faces of adjoining prisms. Larger differences in metal sizes in the four MgBaX phases are better accommodated in the tetragonal anti- PbFCl (Cu_2Sb) structure (3). Although $8 + 1$ coordination in an augmented square antiprism is a common description of the PbFCl structure, this can also be viewed as a distortion

* The Ames Laboratory–DOE is operated for the U.S. Department of Energy by Iowa State University under Contract W-7405-Eng-82. This research was supported in part by the Office of Basic Energy Sciences, Materials Sciences Division.

of the shared tricapped trigonal prisms found in PbCl_2 and other structure types (5). No examples of CaSrX or SrBaX phases are recorded.

These and other phases in the more general $A-A'-X$ systems in which $X-X$ bonding intrudes often show substantial dependence of structure on the relative sizes of A and A' . Our interest in the Mg-Sr-Ge system among these was sparked by the fact that MgSrGe was the only ternary phase reported. Our investigations have shown four other members exist. The two new Zintl phases described here are particularly remarkable in that they are isostructural with metallic transition-metal phosphides originally defined for $\text{Zr}_2\text{Fe}_{12}\text{P}_7$ (6) and for $\text{Ho}_5\text{Ni}_{19}\text{P}_{12}$ (7) or the very closely related $\text{Sc}_5\text{Co}_{19}\text{P}_{12}$ (8). Augmented trigonal prisms about isolated Ge or P atoms that share edges and faces continue to be the dominant structural feature.

Experimental

The synthetic, glove box, Guinier, and single crystal methodologies have all been described before (9). The Mg utilized was Fisher reagent grade in the form of chips, and the Ge was a zone-refined Johnson Matthey product that was ground to a powder and stored in the glove box. The Sr was an Ames Lab vacuum-sublimed product described earlier (9); any oxide coating that developed was cut off in the box. Reagents were weighed to the nearest milligram and loaded into Ta reaction tubes already sealed at one end. These were tightly crimped, Heliarc welded, and then sealed within well-evacuated fused silica jackets for reaction.

Synthesis

The earliest reactions that led to the initial phase identifications were loaded with diverse $A_xA_{2-x}\text{Ge}$ compositions and run at $\sim 910^\circ\text{C}$ for 5–14 days followed by 5–28 days

at $700\text{--}840^\circ\text{C}$. However, phase compositions found were sometimes inconsistent and even impossible, i.e., three or four phases in a supposedly equilibrium system. These problems were overcome by the use of higher temperatures, 1100°C for 2 days, after which that product was usually ground, pressed into a pellet, and further reacted for an additional 17–21 days at $900\text{--}980^\circ\text{C}$. The second step was also applied to products of the earlier, 910°C reactions. All yielded seemingly equilibrium systems and consistent results, whereas the first 1100°C –2-day step was not sufficient unless 7–30 days was applied, at least for Sr-poorer samples. Cold-pressing the elements into pellets and allowing these to react via slow heating to 1000°C over 2 days followed by 10 days more at that temperature seemed to be suitable as well. Small amounts of reaction of Ge with the Ta container in the first step at 1100°C were encountered in a few cases, and wetting of the container wall in the first step sometimes made recovery of all of the products difficult. The new phases are dull to shiny gray and turn yellow-green in the air in 15–20 min.

New Phases

The X-ray powder pattern of $\text{Sr}_2\text{Mg}_{12}\text{Ge}_7$ was first indexed as primitive hexagonal by TREOR (10) (23 lines) for a sample with the overall proportions $\text{Sr}:\text{Mg}:\text{Ge} = 2:10:6$. This result was found to be isostructural with $\text{Zr}_2\text{Fe}_{12}\text{P}_7$ ($P\bar{6}$) (11) based on cell dimensions and the good agreement of the calculated powder pattern. A high yield of a second phase was encountered with higher strontium proportions. Indexing was again provided by TREOR, also as primitive hexagonal, and the similarity of c axis lengths to that of $\text{Sr}_2\text{Mg}_{12}\text{Ge}_7$ and SrMg_3Ge_3 (below) suggested similarly linked trigonal prisms were present. The data were found to be well accounted for by the structure reported for $\text{Ho}_5\text{Ni}_{19}\text{P}_{12}$ ($P\bar{6}2m$) (3). (This assignment cannot be distinguished from that of the

Sc₅Co₁₉P₁₂ (8) type as these differ only in the apparent disorder of one transition metal atom in the latter.) The dimensional variations obtained with different input stoichiometries indicated the phase had an appreciable compositional range.

Variation of the A : Ge ratio to lower values, where polygermanium anions might be expected, also gave two more new phases, but these were not completely characterized. A composition near SrMg₃Ge₃ yielded a sharp pattern, 31 lines from which were indexed by TREOR as primitive orthorhombic ($a = 14.628$ (2) Å, $b = 12.669$ (2) Å, $c = 4.4272$ (5) Å). The dimensions and calculated powder pattern suggested a structural model close to that of Rh₄P₃ (*Pnma*) (11). However, a few lines in the calculated pattern were not observed, and a couple of observed reflections violated systematic absences for this model. Single crystals were not found. The composition SrMg₂Ge₂ also gave a pattern that did not contain any of the known binary or ternary phases and was not close to that for either a ThCr₂Si₂ or a CaBe₂Ge₂ type structure. No further progress was made.

Crystallography

Rod-like crystals were isolated from a sample near the composition Sr₂Mg₁₂Ge₇ that had been reacted 1 week each at 900 and 800°C and consisted (according to the powder pattern) of about 70% of this phase and 30% of Sr₅Mg₁₉Ge₁₂. Weissenberg photographs of *hk0*, *hk1* and *hk2* layers indicated a hexagonal cell with no systematic absences, and no mirror plane was apparent perpendicular to the *c* axis. The *P6* space group reported for the seemingly isostructural Zr₂Fe₁₂P₇ (7) was considered appropriate. An absorption correction with both θ and ψ dependence was applied to the data based on eight ψ -scans. Averaging in *6/m* Laue symmetry (7.0 and 4.2% based on *I* and *F*, respectively) was much better than in *6/mmm*.

The original model did not refine very well. Direct methods (SHELX-86) (12) gave several Sr and Ge peaks that were close to those of the model, and subsequent difference mapping located the remainder. The difference was found to result from an alternative orientation of the cell. Electron density at the Mg4 position seemed excessive so the occupancies of all Sr and Mg atoms were first refined relative to Ge. Only the variation at Mg4 was significant, giving 112.4(8)% Mg occupancy or a cell composition (based on neutral atoms) of Sr_{2.17(2)}Mg_{11.83(2)}Ge, with the likely, full occupancy of the site assumed. However, small negative peaks of ~ 1.3 e/Å³ were present at both of the Sr positions in the final ΔF map, corresponding to ~ 0.05 Mg, 0.95 Sr at each, so the deviation from the stoichiometric formula may not be so large. The residuals *R* and *R_w* at convergence were 2.7 and 4.2% based on *F*. Refinement of the alternate enantiomorph gave higher residuals, 2.8 and 4.6%.

Some diffraction and refinement data are summarized in Table I. The atom parameters and important distances are given in Tables II and III, respectively, for a cell with the same orientation as originally reported (6). Tables of anisotropic thermal parameters and of *F_o*/*F_c* are available from J.D.C.

Results and Discussion

The three ternary phases in the Sr_{*x*}Mg_{2-*x*}Ge section have the ideal compositions and structure types MgSrGe—inverse PbCl₂ (4), Sr₂Mg₁₂Ge₇—Zr₂Fe₁₂P₇ (6), and Sr₅Mg₁₉Ge₁₂—Ho₅Ni₁₉P₁₂ (7) or Sc₅Co₁₉P₁₂ (8). The end members are Mg₂Ge (CaF₂⁻¹) and Sr₂Ge (PbCl₂⁻¹), respectively (3). The first synthetic explorations suggested that each of the two new phases exhibited a significant nonstoichiometry, and so a series of 1100°C reactions followed by 900–980°C equilibrations were carried out to clarify

TABLE I
CRYSTAL DATA FOR $\text{Sr}_{2.17(2)}\text{Mg}_{11.83(2)}\text{Ge}_7$

Space group, Z	$P\bar{6}$ (No. 174), 1	
a, b (Å)	11.0582 (6) ^a	11.064 (1) ^b
c	4.3530 (4)	4.356 (1)
V (Å ³)	460.99 (5)	461.8 (2)
Crystal dimensions (mm)	0.40 × 0.10 × 0.05	
Data collection instrument	Enraf-Nonius CAD 4	
Radiation	MoK α	
$2\theta_{\text{max}}$ (deg.)	65.0	
Scan mode	$2\theta - \omega$	
Octants	$hkl, \bar{h}kl$	
Reflections		
Measured	1926	
Observed ($I > 3\sigma_I$)	1681	
Independent	517	
Absorption coefficient μ (cm ⁻¹)	170.4	
Range of transmission coefficient	0.53–1.00	
R_{ave} (%)	7.0	
R^c (%)	2.7	
R_w^c (%)	4.2	
Largest residue peak ($e^-/\text{Å}^3$)	–1.35, +1.15	
Second ext. coefficient (10^{-7})	10.0(5)	
No. of variables	48	

^a Refined from 25 high angle reflections on the CAD 4.

^b Refined from 54 Guinier powder pattern reflections with the aid of Si as an internal standard ($\lambda = 1.540562$ Å).

^c Based on F ; $\omega = [\sigma_F]^{-2}$.

TABLE II
POSITIONAL AND ISOTROPIC EQUIVALENT THERMAL PARAMETERS FOR $\text{Sr}_{2.17}\text{Mg}_{11.83}\text{Ge}_7$ (SPACE GROUP $P\bar{6}$)

Atoms	Site	x	y	z	$B(\text{Å}^2)$
Sr1	1c	$\frac{1}{3}$	$\frac{2}{3}$	0	1.16 (2)
Sr2	1f	$\frac{2}{3}$	$\frac{1}{3}$	$\frac{1}{2}$	1.26 (2)
Ge1	3j	0.41632 (9)	0.2970 (1)	0	0.97 (2)
Ge2	3k	0.12166 (8)	0.4120 (1)	$\frac{1}{2}$	0.94 (2)
Ge3	1a	0	0	0	1.52 (2)
Mg1	3j	0.4272 (4)	0.0550 (3)	0	1.15 (6)
Mg2	3j	0.1603 (4)	0.2771 (3)	0	1.13 (5)
Mg3	3k	0.3882 (3)	0.4310 (4)	$\frac{1}{2}$	0.98 (6)
Mg4 ^a	3k	0.2158 (3)	0.0926 (4)	$\frac{1}{2}$	1.66 (6)

^a Occupancy refined to 94.3 (4)% Mg, the remainder Sr.

TABLE III
 IMPORTANT DISTANCES (Å) AND ANGLES (DEG) IN $\text{Sr}_{2.2}\text{Mg}_{11.8}\text{Ge}_7^a$

Atom 1	Atom 2		Distance	Atom 1	Atom 2		Distance
Ge1	Mg1	1 ×	2.739 (4)	Ge3	Mg2	3 ×	2.665 (3)
Ge1	Mg1	1 ×	2.764 (4)	Ge3	Mg4	6 ×	3.006 (2)
Ge1	Mg2	1 ×	2.727 (4)	Mg1	Mg2	1 ×	3.046 (4)
Ge1	Mg3	2 ×	2.737 (2)	Mg1	Mg3	2 ×	3.172 (4)
Ge1	Mg4	2 ×	3.123 (3)	Mg2	Mg3	2 ×	3.114 (4)
Ge1	Sr2	2 ×	3.3839 (5)	Mg1	Sr2	2 ×	3.616 (2)
Ge2	Mg1	2 ×	2.808 (2)	Mg3	Sr1	2 ×	3.671 (3)
Ge2	Mg2	2 ×	2.790 (2)				
Ge2	Mg3	1 ×	2.751 (4)				
Ge2	Mg3	1 ×	2.848 (2)				
Ge2	Mg4	1 ×	2.872 (3)				
Ge2	Sr1	2 ×	3.3993 (8)				

Atom 1	Atom 2	Atom 3	Angle
Mg1	Ge1	Mg2	118.17 (9)
Mg1	Ge1	Mg3	70.42 (9)
Mg3	Ge1	Mg3	105.35 (8)
Mg3	Ge1	Mg4	66.89 (10)
Mg1	Ge2	Mg1	101.61 (6)
Mg1	Ge2	Mg2	65.95 (8)
Mg1	Ge2	Mg3	69.57 (8)
Mg2	Ge2	Mg2	102.51 (8)
Mg3	Ge2	Mg3	132.25 (10)
Mg4	Ge3	Mg4	92.78 (6)
Ge2	Sr1	Ge2	79.64 (2)
Mg1	Sr1	Mg2	47.09 (7)
Ge1	Sr2	Ge1	80.06 (1)
Mg3	Sr2	Mg4	46.78 (8)
Sr1	Mg1	Mg2	64.01 (8)
Sr1	Mg2	Mg1	68.94 (9)
Sr2	Mg3	Mg4	76.16 (8)
Sr2	Mg4	Mg3	57.06 (7)

^a Only the shortest Mg–Mg and Mg–Sr distances are listed.

this. Some of the earlier variability was evidently caused by incomplete reactions and gross sample inhomogeneities, particularly for phases with local compositions that did not lie within the $\text{Sr}_x\text{Mg}_{2-x}\text{Ge}$ section. A significant compositional variable actually applies only to the $\text{Sr}_5\text{Mg}_{19}\text{Ge}_{12}$ phase, while the nominal $\text{Sr}_2\text{Mg}_{12}\text{Ge}_7$ is a line phase at 980°C as judged by the invariability of the Guinier-based lattice dimensions within 3 σ limits.

The lattice constants for samples $\text{Sr}_{5+y}\text{Mg}_{19-y}\text{Ge}_{12}$ equilibrated at 980°C (1100°C at the upper limit) shown in Fig. 1 enable us to put limits of about $-0.7 \leq y \leq 2.7$ on the stoichiometry. The former extends nearly to the $\text{Sr}_{2.2}\text{Mg}_{11.8}\text{Ge}_7$ phase, which corresponds to $y = -1.3$ on this scale. The dimensions at the ideal ($y = 0$) composition are about $a = 14.67$, $c = 4.434$ Å presuming the loaded compositions remained accurate. The 53 observed reflections in its powder

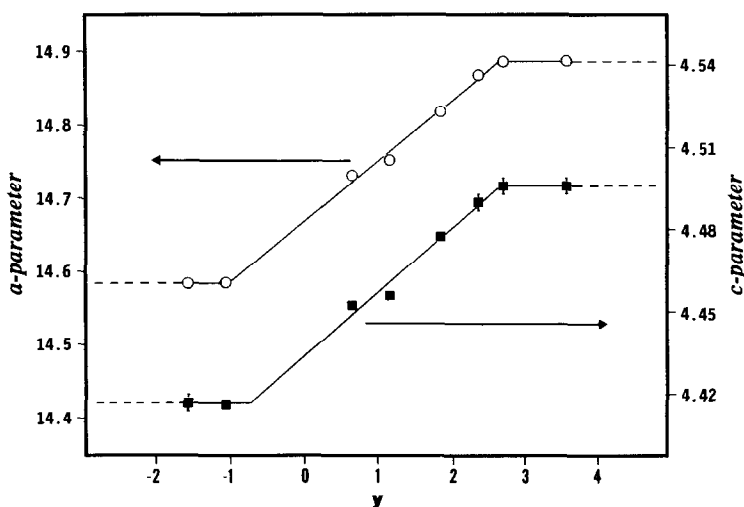


FIG. 1. Lattice parameters vs strontium content based on the formula $\text{Sr}_{5+y}\text{Mg}_{19-y}\text{Ge}_{12}$. The 3σ error limits where not shown were less than the symbol sizes. Only the three samples with data lying on the horizontal lines were biphasic by X-rays.

pattern were in excellent agreement in both positions and intensities with those calculated on the basis of the observed lattice constants and the atom coordinates reported for $\text{Ho}_5\text{Ni}_{19}\text{P}_{12}$ (7). The structure is considered below.

The evident line phase $\text{Sr}_{2.17(2)}\text{Mg}_{11.83(2)}\text{Ge}_7$ has a slightly off-stoichiometry version of the structure originally reported for $\text{Zr}_2\text{Fe}_{12}\text{P}_7$. The refined structure of the former is illustrated in Fig. 2 in a version that emphasizes the common trigonal prismatic arrangement of Mg (crossed ellipsoids) and Sr (open ellipsoids) about Ge (shaded ellipsoids). This coordination is in all cases augmented by three additional Mg atoms that lie in the same plane as Ge and outside of the rectangular faces of each prism. The Sr1 atom is seen to lie at the juncture of a fan-shaped array of three trigonal prisms about Ge2 that share the Sr1–Sr1 edge along $\frac{1}{3}$, $\frac{2}{3}$, z (Fig. 2). The Mg1 and Mg2 atoms in these each bond to Ge in two adjoining prisms through prism faces as well as to Ge2, resulting in an approximately tetrahedral environment. Such “fans” at Sr2 ($\frac{2}{3}$,

$\frac{1}{3}$, $\frac{1}{2}$) are part of rings of nine prisms sharing edges that branch at Sr2.

Figure 3 shows a [001] section of the same structure one cell deep with differentiation

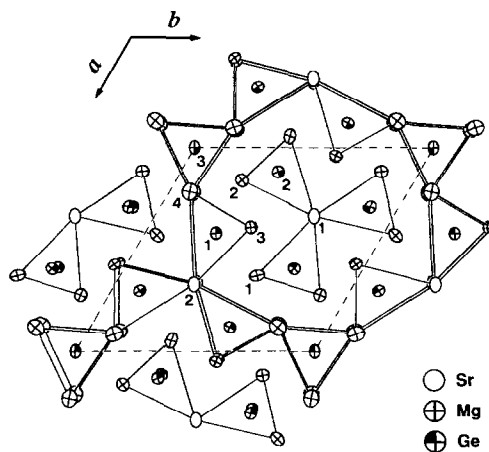


FIG. 2. [001] projection of the structure of $\text{Sr}_{2.2}\text{Mg}_{11.8}\text{Ge}_7$ ($\text{Zr}_2\text{Fe}_{12}\text{P}_7$ type) with lines emphasizing the tricapped trigonal prisms about germanium atoms. Sr, open ellipsoids; Mg, crossed ellipsoids, Ge, shaded ellipsoids (95% probability level). All atoms lie at $z = 0$ or $\frac{1}{2}$.

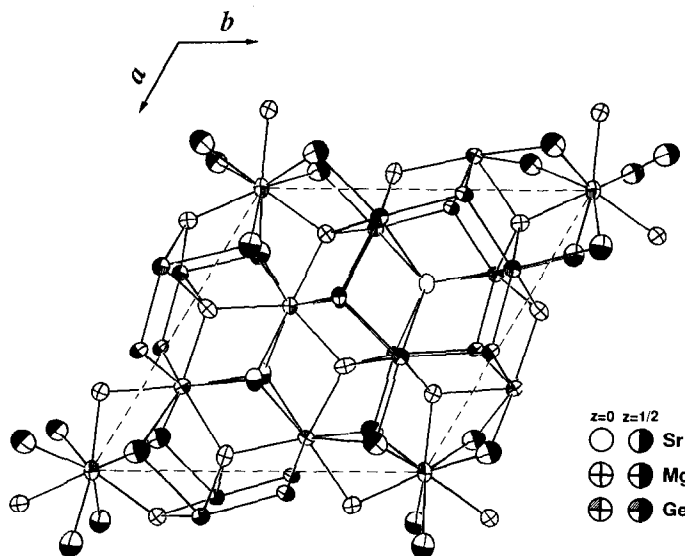


FIG. 3. [001] projection of the structure of $\text{Sr}_{2.2}\text{Mg}_{11.8}\text{Ge}_7$ emphasizing the Ge–Mg and Ge–Sr interactions that lead to tricapped trigonal prismatic arrangements about germanium. The atoms are keyed by type and height in z , as in Fig. 2.

between atoms that lie at $z = 0, 1$ and at $z = \frac{1}{2}$ (half shaded). In order to emphasize bonding, the lines in this figure mark instead the Ge–Mg, Sr interactions within the trigonal prisms together with the Ge–Mg bonds through the prismatic faces. The structure is continuous along c as the trigonal prisms all share both end faces.

The partial occupation of the Mg4 site by $\sim 5.7\%$ Sr occurs about the Ge3 site which has greatest “Mg”–Ge distances. This is also the only site in the structure where Mg is five-coordinate (roughly square pyramidal) rather than tetrahedral. The disorder is presumably responsible for the fact that Mg4 (+Sr) and Ge3 exhibit the largest thermal parameters in the structure. The other three Mg atoms about each Ge that cap rectangular faces of all trigonal prisms are at substantially the same Mg–Ge distances as within the prism, i.e., the nine-coordination is quite regular. The average $d(\text{Ge–Mg})$, excepting those about Mg4, is 2.76 \AA , the same as in Mg_2Ge (3), the Ge–Mg4 separations are 3.04 \AA , and $d(\text{Ge–Sr})$ is 3.39 \AA .

A projection of the structure of the other new phase, the nominal $\text{Sr}_5\text{Mg}_{19}\text{Ge}_{12}$, is shown in Fig. 4 (after $\text{Ho}_5\text{Ni}_{19}\text{P}_{12}$ (7)), where Sr, Mg, and Ge are identified as large, medium, and small circles, respectively, and are shaded according to height. Comparison with Fig. 2 shows some similar elements but with more heavily linked prisms, including shared faces. The locale of the predominant Sr-rich nonstoichiometry of $\text{Sr}_5\text{Mg}_{19}\text{Ge}_{12}$ can be readily predicted on the basis of the behavior of $\text{Sr}_{2.2}\text{Mg}_{11.8}\text{Ge}_7$. The substitution of Sr for Mg is expected to occur first on the Mg4 (Ni4) site, a distinctly larger site in which Mg (Ni) again has five rather than four Ge (P) neighbors, and an incomplete structural study of the phase confirms this. The nature of the inverse substitution is not as obvious based on the data for $\text{Ho}_5\text{Ni}_{19}\text{P}_{12}$ or $\text{Sc}_5\text{Co}_{19}\text{P}_{12}$, where nonstoichiometry was not encountered. Pivan *et al.* (7) have published a broader comparison of these two structures with other types, including a Zintl phase analogue we did not see,

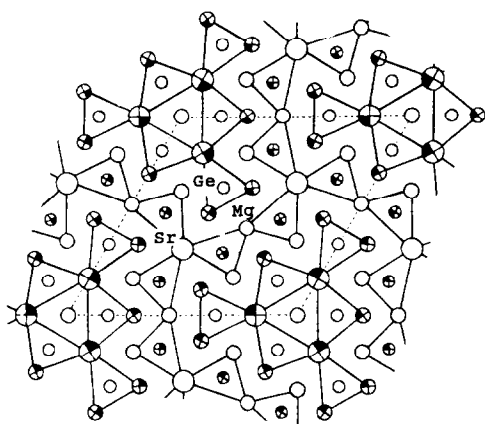


FIG. 4. The ideal structure of $\text{Sr}_5\text{Mg}_{19}\text{Ge}_{12}$ based on the parameters for $\text{Ho}_5\text{Ni}_{19}\text{P}_{12}$ (7). The lines emphasize trigonal prisms about germanium. Ge, Mg, and Sr are marked by small, medium, and large circles, respectively, with open atoms at $z = 0$, shaded atoms at $z = \frac{1}{2}$. (Compare Fig. 2.)

$\text{Zr}_6\text{Ni}_{20}\text{P}_{13}$, which has the same metal : non-metal ratio as $\text{Zr}_2\text{Ni}_{12}\text{P}_7$.

These two structure types illustrate a commonality of augmented trigonal prismatic coordination in cases where there is strong polar covalent bonding between a metalloid and relatively electropositive elements. A size distinction between the two cations clearly allows greater versatility. The new $\text{Sr}_5\text{Mg}_{19}\text{Ge}_{12}$ is a structural member of a fairly large series of phosphides: $\text{Ho}_5\text{Ni}_{19}\text{P}_{12}$ (7) and the very closely related $\text{Ln}_5\text{Co}_{19}\text{P}_{12}$ (8, 13), $\text{Ln}_5\text{Ru}_{19}\text{P}_{12}$ (14), both with a considerable range of Ln ($\text{Ln} = \text{lanthanide, Y, Sc}$), and $\text{Zr}_5\text{Co}_{19}\text{P}_{12}$ (15). The $\text{Zr}_2\text{Fe}_{12}\text{P}_7$ type appear even more widespread. One large group has many $\text{Ln}_2(\text{Fe, Co, Ni})_{12}(\text{P, As})_7$ combinations (16–18), all of which appear to be stoichiometric and are doubtlessly metallic. An extensive magnetic study has also appeared (19). On the other hand, a family of group II analogues with this structure, $(\text{Mg, Ca})_{2+x}\text{Ni}_{12-x}(\text{P, As})_7$ (20–22), are distinctly off-stoichiometry, with cation mixing in the same A4 site yielding compositions in the range of 0.1 \leq

$x \leq 0.5$ in different examples, as found with $\text{Sr}_{2.2}\text{Mg}_{11.8}\text{Ge}_7$.

The new compounds $\text{Sr}_{2.2}\text{Mg}_{11.8}\text{Ge}_7$ and $\text{Sr}_5\text{Mg}_{19}\text{Ge}_{12}$ are the first nonpnictide examples of these structure types. They are Zintl compounds as well where only metallic phases had been known before. Clearly the requirements of strong, ninefold bonding about the metalloid and favorable geometries achieved therewith in the presence of two different cation sizes are the most important features of these structures, while, as often observed, the electronic requirements of the additional conduction electrons in the pnictide examples appear less important. It is interesting to note, with hindsight, that the above group of calcium or magnesium nickel phosphides and arsenides have seven electrons per formula unit in a presumably metal-based conduction band if nickel is taken to be dipositive. The formation of the present germanium phases might have been predicted on this basis. The silicides can presumably also be achieved.

Acknowledgments

S.J.S. was supported in part by the National Science Foundation, Solid State Chemistry, via Grant DMR-8902954.

References

1. E. ZINTL, *Angew. Chem.* **52**, 1 (1939).
2. H. SCHÄFER, B. EISENMANN, AND W. MÜLLER, *Angew. Chem. Intl. Ed. Eng.* **12**, 694 (1973).
3. P. VILLAR AND L. D. CALVERT, "Pearson's Handbook of Crystallographic Data for Intermetallic Phases," Vols. 1–3, Amer. Soc. Met: Metals Park, Ohio (1985).
4. B. EISENMANN, H. SCHÄFER, AND A. WEISS, *Z. Anorg. Allg. Chem.* **391**, 241 (1972).
5. B. G. HYDE AND S. ANDERSSON, "Inorganic Crystal Structures," p. 81, Wiley, New York (1989).
6. E. GANGLBERGER, *Monatsh. Chem.* **99**, 557 (1968).
7. J. Y. PIVAN, R. GÜERIN, AND M. SERGENT, *Inorg. Chem. Acta* **109**, 221 (1985).
8. W. JEITSCHKO AND E. J. REINBOLD, *Z. Naturforsch. B* **40**, 900 (1985).
9. W.-M. HURNG AND J. D. CORBETT, *Chem. Mater.* **1**, 311 (1989).
10. P. E. WERNER, "TREOR-4 Trial and Error Pro-

- gram for Indexing Unknown Powder Patterns," Department of Structural Chemistry, Arrhenius Laboratory, University of Stockholm, 106 91 Stockholm, Sweden (1984).
11. S. RUNDQVIST AND A. HEDE, *Acta Chem. Scand.* **14**, 893 (1960).
 12. G. M. SHELDRIK, "SHELXS-86, Programs for Structure Determination," University of Göttingen, Germany, 1986.
 13. U. JAKUBOWSKI-RIPKE AND W. JEITSCHKO, *J. Less-Common Met.* **136**, 261 (1988).
 14. V. GHETTA, P. CHAUDOUËT, R. MADAR, J. P. SENATEUR, AND B. LAMBERT-ANDRON, *J. Less-Common Met.* **146**, 299 (1989).
 15. V. GHETTA, P. CHAUDOUËT, R. MADAR, J. P. SENATEUR, AND B. LAMBERT-ANDRON, *J. Less-Common Met.* **120**, 197 (1986).
 16. W. JEITSCHKO, D. J. BRAUN, R. H. ASHCRAFT, AND R. MARCHAND, *J. Solid State Chem.* **25**, 309 (1978).
 17. W. JEITSCHKO AND B. JABERG, *Z. Anorg. Allg. Chem.* **467**, 95 (1980).
 18. W. JEITSCHKO AND B. JABERG, *J. Less-Common Met.* **79**, 311 (1981).
 19. M. REEHUIS AND W. JEITSCHKO, *J. Phys. Chem. Solids* **50**, 563 (1989).
 20. A. MEWIS, *Z. Naturforsch. B.* **32**, 351 (1977).
 21. A. MEWIS AND A. DISTLER, *Z. Naturforsch. B.* **35**, 391 (1980).
 22. A. MEWIS, *Z. Naturforsch. B.* **35**, 620 (1980).